

## Buffer-Induced Swelling and Vesicle Budding in Binary Lipid Mixtures of Dioleoylphosphatidylcholine:Dioleoylphosphatidylethanolamine and Dioleoylphosphatidylcholine:Lysophosphatidylcholine Using Small-Angle X-ray Scattering and $^{31}\text{P}$ Static NMR

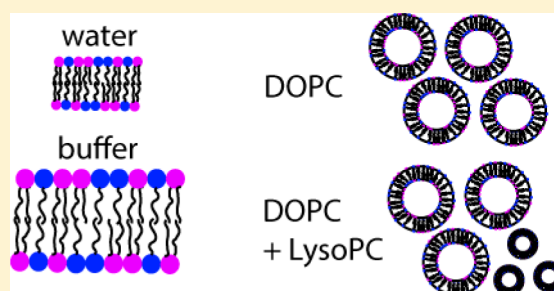
Hanna M. G. Barriga,<sup>†</sup> Richard Bazin,<sup>‡</sup> Richard H. Templer,<sup>†</sup> Robert V. Law,<sup>\*,†</sup> and Oscar Ces<sup>\*,†</sup>

<sup>†</sup>Department of Chemistry, Imperial College London, London, SW7 2AZ, United Kingdom

<sup>‡</sup>Pfizer Global Research and Development, Sandwich, Kent CT13 9NJ, United Kingdom

### Supporting Information

**ABSTRACT:** A large variety of data exists on lipid phase behavior; however, it is mostly in nonbuffered systems over nonbiological temperature ranges. We present biophysical data on lipid mixtures of dioleoylphosphatidylcholine (DOPC), dioleoylphosphatidylethanolamine (DOPE), and lysophosphatidylcholine (LysoPC) examining their behaviors in excess water and buffer systems over the temperature range 4–34 °C. These mixtures are commonly used to investigate the effects of spontaneous curvature on integral membrane proteins. Using small-angle X-ray scattering (SAXS) and  $^{31}\text{P}$  NMR, we observed lamellar and vesicle phases, with the buffer causing an increase in the layer spacing. Increasing amounts of DOPE in a DOPC bilayer decreased the layer spacing of the mesophase, while the opposite trend was observed for increasing amounts of LysoPC.  $^{31}\text{P}$  static NMR was used to analyze the DOPC:LysoPC samples to investigate the vesicle sizes present, with evidence of vesicle budding observed at LysoPC concentrations above 30 mol %. NMR line shapes were fitted using an adapted program accounting for the distortion of the lipids within the magnetic field. The distortion of the vesicle, because of magnetic susceptibility, varied with LysoPC content, and a discontinuity was found in both the water and buffer samples. Generally, the distortion increased with LysoPC content; however, at a ratio of DOPC:LysoPC 60:40, the sample showed a level of distortion of the vesicle similar to that of pure DOPC. This implies an increased flexibility in the membrane at this point. Commonly, the assumption is that for increasing LysoPC concentration there is a reduction in membrane tension, implying that estimations of membrane tension based on spontaneous curvature assumptions may not be accurate.



### ■ INTRODUCTION

Biological membranes are composed of a complex mixture of lipids and proteins; however, phospholipids form the main component.<sup>1</sup> There has for a long time been interest into how lipids and membrane proteins interact and how this can be quantified. To date, there are a variety of studies on different proteins looking at the direct effects of membranes on those proteins. A few examples are the effects of membranes on diacylglycerol kinase,<sup>2,3</sup> bacteriorhodopsin,<sup>4</sup> and CTP:phosphatidylcholine cytidyltransferase.<sup>5</sup>

Here, we focus on mixtures of dioleoylphosphatidylcholine (DOPC) combined with dioleoylphosphatidylethanolamine (DOPE) or lysophosphatidylcholine (LysoPC). Structures for these lipids can be seen in Figure 1. These specific combinations are particularly interesting as they are often used for probing the effects of spontaneous curvature on lipid mixtures.<sup>6</sup> While there are some investigations on the phase behavior of these systems,<sup>7,8</sup> there is less information on the systems in biologically inspired buffers at excess hydrations

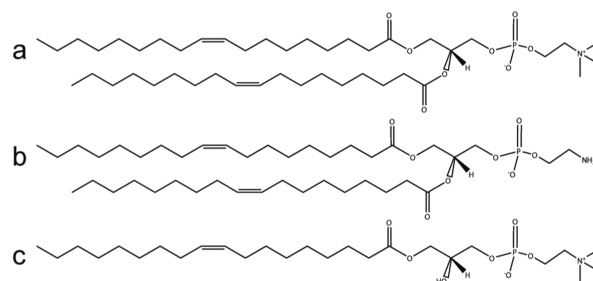


**Figure 1.** Structures for (a) DOPC, (b) DOPE, and (c) LysoPC.

(above 70 % wt/wt) and also over temperature ranges relevant to biological assays. Understanding, in more depth, the fundamental properties of the lipids within the membranes

**Received:** December 10, 2014

**Revised:** January 23, 2015

**Published:** March 4, 2015

and how the different compositions, temperatures, and hydration media can cause variation in the membranes is important if future studies are to be used to identify specific protein behaviors.

In an aqueous environment, lipids are driven by the hydrophobic effect to form mesophases. Their compositions and geometry influence the energetically favorable phases they form, as they arrange themselves to minimize exposure of their hydrophobic parts.<sup>9</sup> Many factors influence lipid phase behavior including lipid geometry, temperature, pressure, hydrating medium, and level of hydration. Generally, lyotropic liquid crystals will swell up to a limiting point, known as the excess water point. This point has been shown to differ according to lipid structure and charge and also to decrease at lower temperatures.<sup>10</sup> It is possible to determine the excess water point of a lipid sample by fitting the swelling curve which is the change in layer spacing with respect to the water content of the sample. Generally, the layer spacing increases linearly up to a point, after which it will plateau. If a straight line is fitted to the linear swelling data and to the data which has plateaued, then the intersection of the two lines can be defined as the excess water point. In this study, all lipids were measured at a hydration well above the excess water in order to facilitate the best possible comparison with biological systems. Using biological levels of hydration would have resulted in a level of signal reduction below acceptable experimental levels.

Transverse and lateral interactions within the membrane also play a highly important role in phase changes and stability and can be affected by the aqueous solution the lipid is hydrated in. The lateral interactions can be divided into three main regions: headgroups, interfaces, and chains. The electrostatic repulsions between polar headgroups and repulsive hydration forces are counteracted by a strong hydrophobic effect, causing the headgroups to bunch together to minimize the exposure of the chains to water. In addition to this, repulsive steric interactions between the hydrocarbon chains are counteracted by van der Waals forces and hydrogen bonding between chains. Transverse interactions can occur with the surrounding media or with adjacent lipid bilayers, emphasizing the importance of the hydration media.<sup>5</sup> It has in fact been shown that the presence of buffers with high salt content can affect the swelling profile of a charged bilayer by charge screening and weakening the electrostatic repulsion between layers.<sup>11</sup> Additionally, there have been limited reports of biological buffers affecting the mechanical properties of bilayers, although the exact mechanisms have not yet been studied in detail.<sup>12,13</sup> For these reasons, the extensive work undertaken was performed in both water and buffer to enable the decoupling of lipid composition effects from the buffers.

Small-angle X-ray scattering (SAXS) was used to determine the phase behavior of the lipid mixtures and the effects of buffer on the swelling of the bulk mesophase. Many protein reconstitution studies are carried out at 4 °C followed by subsequent activity measurements at room temperature.<sup>14–17</sup> There is, however, little knowledge about the effects of these conditions on the lipid systems. This motivated a temperature range of 4–34 °C for these investigations with the upper limit of temperature as an overestimation of room temperature and close to physiological temperature. We present SAXS data spanning the compositional range of DOPC:DOPE and DOPC:LysoPC from 100:0 up to a 50:50 molar ratio in excess water and buffer systems. Specifically, this combination of lipids and buffer mirrors compositions used to investigate the effects

of spontaneous curvature and membrane mechanics on protein activity.<sup>6,18,19</sup>

In addition, the DOPC:LysoPC mixtures have been probed using <sup>31</sup>P static NMR. LysoPC is a type I lipid,<sup>5</sup> particularly known for its ability to curve toward the interface and therefore to cause the formation of micelles or vesicle budding<sup>20</sup> when incorporated into lipid vesicles. <sup>31</sup>P static NMR was performed to establish if there is a single phase in the bulk mesophase mixtures, a key factor if the lipids are being used for protein activity studies. The results expected from a protein reconstituted into a micelle would be expected to be widely different from one reconstituted into a vesicle;<sup>21,22</sup> hence, an understanding is needed to establish if micellar formation occurs and at which point it may start to affect any protein activity assay results. Another key aspect of the NMR data is the ability to map changes in the deformation of the membrane with varying lipid compositions by fitting the NMR line shapes. This is crucial data as protein activity and conformation are known to be influenced by membrane tension,<sup>18,23</sup> and hence, variations in this as a result of lipid composition must be understood in greater detail. These experiments were again carried out above the excess hydration point and in both water and buffer.

In summary, we have used SAXS to investigate the effects of buffer on phase behavior and layer spacing, combined with NMR to determine vesicle budding and changes in the susceptibility of the membrane for deformation.

## ■ EXPERIMENTAL SECTION

**Materials.** All the lipids were purchased from Avanti Polar Lipids (Alabaster, AL, U.S.) in lyophilized powder form and were delivered with a purity of >99%, and so no further purification was necessary. To ensure the samples were dry, they were placed on a lyophilizer (Thermo Scientific, Asheville, NC, U.S.) for a further 12 h before use. The lipids used were 1,2-dioleoyl-*sn*-glycero-3-phosphocholine (DOPC), 1-oleoyl-2-hydroxysn-glycero-3-phosphocholine (LysoPC), and 1,2-dioleoyl-*sn*-glycero-3-phosphatidylethanolamine (DOPE). Lipid mixtures were made by codissolving the relevant lipids in chloroform purchased from Sigma-Aldrich (Gillingham, Dorset, U.K.) and then by drying the samples under a stream of nitrogen gas. Samples were lyophilized again for a minimum of 12 h after which they were sealed and stored at –20 °C. The buffer used to hydrate the lipid samples was 20 mM 4-(2-hydroxyethyl)piperazine-1-ethanesulfonic acid (HEPES), 100 mM KCl, 0.5 M sucrose, pH 7.2, in Milli-Q (MQ) water and was sterile filtered before being stored at 4 °C. All the materials for this buffer were purchased from Sigma-Aldrich.

**X-ray Sample Preparation.** X-ray and NMR samples were removed from the –20 °C freezer and were allowed to adjust to room temperature before being hydrated either in MQ water or in buffer on a w/w basis to a minimum of 70 wt % hydration. They were then sealed, freeze-thawed, and vortexed four times using liquid nitrogen and hot air. Afterward, samples were left overnight to equilibrate at 4 °C before being transferred to the sample holders and being measured. This additional equilibration step was performed as varying equilibration times were observed for different lipid mixtures and the overnight equilibration ensured that they were all fully equilibrated when measured.

**Sample Hydration.** The use of 70 wt % hydration was chosen from prior determination of the excess water point by fitting swelling curves for a selection of the compositions, after which the hydration was chosen to be a minimum of 5 wt % above the excess water point. For a temperature increase of 45 °C, the number of water molecules required for each DOPC lipid to be in excess hydration only increases by five water molecules. Other lipids also exhibit similar behavior.<sup>10</sup> Therefore, assuming a minimum of an increase of 10 water molecules for each lipid over a 45 °C temperature change, and using an initial

sample hydration of 60%, this only corresponds to a change in the excess hydration point of 3.3%. Hence, the use of a minimum of 5% above the excess water point is justified.

**Experimental Setup.** X-ray samples were acquired using two X-ray beamlines: ID02 at the European Synchrotron Radiation Facility (ESRF) and an in-house BEDE Microsource Generator. The ESRF data was taken at a wavelength of 0.73 Å with samples contained in Teflon spacers sealed with mylar windows. The in-house system operates at 1.54 Å with samples run in sealed glass capillaries. A selection of samples was run on both beamlines to check consistency and was found to be in good agreement. Example images have been included in Figure S1 of the Supporting Information for DOPC:DOPE and DOPC:LysoPC mixtures at differing temperatures.

NMR spectra were recorded on a Bruker DRX 600 MHz NMR spectrometer operating at 14.09 T with a  $^{31}\text{P}$  resonance of 242.9 MHz. This was carried out using a 4 mm double bearing probe, with a pulse length of 4  $\mu\text{s}$  90° pulse using a Bloch decay method. Samples were loaded into a 4 mm zirconia rotor, were sealed with a Kel-F end-cap, and were left overnight at 4 °C to equilibrate. NMR line shapes were fitted using a Matlab program as outlined in the Introduction section. All of the fits had an  $R^2$  value of 0.96 or greater. Example fits can be found in Figure S2 of the Supporting Information. For samples showing a significant isotropic component, an isotropic Gaussian peak centered at 0 ppm was added to the fitting process to account for this.

**NMR Data Fitting.**  $^{31}\text{P}$  static NMR spectra were fitted using a Matlab program built to take into account the effects of magnetic susceptibility<sup>24</sup> distortions of vesicles in a magnetic field on the line shape. The line shape of a  $^{31}\text{P}$  static NMR spectrum for phospholipid liposomes is governed by its shielding tensor and the orientation of the phospholipids within the magnetic field. Because of magnetic susceptibility effects, phospholipid molecules have a tendency to orient with their long axis perpendicular to the magnetic field, which results in a deformation of the liposomes to ellipsoids.<sup>25</sup> The extent of this deformation is described by the ratios of the two perpendicular axes of the ellipsoid, also known as the  $c/a$  parameter (Figure 2).

The  $c/a$  parameter depends upon curvature elastic properties of the membrane via<sup>24</sup>

$$c - a = r_0^3 \frac{H^2 \Delta\chi}{12K} \quad (1)$$

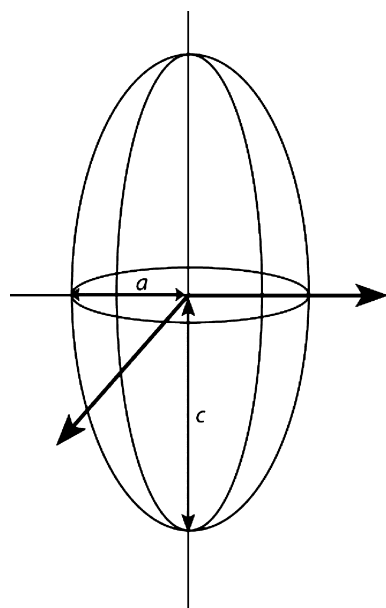


**Figure 2.** A schematic of the distortion of a vesicle because of the magnetic susceptibility in a magnetic field. The lengths,  $a$  and  $c$ , are the axis minimum and maximum, respectively, of the ellipsoid. Image adapted from Picard et al.<sup>25</sup>

where  $r_0$  is the radius of nondeformed liposome in centimeters,  $\Delta\chi$  is the molecular diamagnetic anisotropy of the phospholipid molecules,  $K$  is the curvature elastic modulus in  $10^{-5}$  newtons, and  $H$  is the intensity of the static magnetic field in  $10^{-4}$  tesla. Dubinnyi et al.<sup>24</sup> have proposed an analytical formula for modeling the line shape of  $^{31}\text{P}$  static NMR spectra taking into account deformations caused by the magnetic field and extracting the chemical shielding tensor parameters and the  $c/a$  parameter. The formula has been outlined here as the final line shape function which was used for data fitting, but for more detail, refer to Dubinnyi et al.<sup>24</sup> In this model, the line shape of an anisotropic NMR spectrum of a spin  $1/2$  nucleus is calculated by convolution of a broadening function  $I(\nu)$  with a probability function  $P(\nu)$ . The model then uses a Lorentzian shape for  $I(\nu)$  where the real and imaginary parts correspond to the pure absorption and dispersion parts of the spectrum, respectively. The probability function represents the probability density function of a surface element of the bilayer to be oriented at a fixed angle to the applied magnetic field and therefore to resonate at frequency  $\nu$ . In this case, it is determined by the angular distribution of phospholipid molecules over the surface of the ellipsoid of revolution. Taking into account normalization factors and a transformation into angular space, the line shape can then be expressed as

$$S(\nu) = \frac{i}{\pi} \frac{A}{C - AB} \left( 1 + \frac{2C}{C - AB} \frac{\sqrt{A} \arctan \sqrt{A} - \sqrt{\frac{C}{B}} \arctan \sqrt{\frac{C}{B}}}{\sqrt{A} \arctan \sqrt{A} + \frac{A}{1+A}} \right) \quad (2)$$

This equation describes the line shape as a function of the frequency  $\nu$ ; however, the same equation describes this line shape as a function of chemical shift  $\sigma$  where  $\beta'$  is the Lorentzian broadening factor in ppm and  $A$ ,  $B$ , and  $C$  are described by

$$\begin{aligned} A &= \left( \frac{c}{a} \right)^2 - 1 \\ B &= -\sigma + \sigma_{\text{perp}} - i\beta' \\ C &= \sigma_{\text{para}} - \sigma_{\text{perp}} \end{aligned} \quad (3-5)$$

where  $\sigma_{\text{para}}$  and  $\sigma_{\text{perp}}$  are the parallel and perpendicular components of the chemical shift. This set of equations enabled efficient analysis of  $^{31}\text{P}$  static NMR data using the Levenberg-Marquardt minimization method.<sup>26</sup>

## RESULTS AND DISCUSSION

We first discuss the SAXS data obtained for the lipid mixtures in water and buffer, presenting ideas for the differences seen in the two systems and the effects of increasing concentrations of LysoPC or DOPE in a DOPC bilayer. This investigation then leads into the further analysis of the DOPC:LysoPC samples to identify the isotropic content using  $^{31}\text{P}$  static NMR and the results found from fitting the line shapes to take account of the deformation of the lipids within the magnetic field.

**SAXS Studies on DOPC:DOPE and DOPC:LysoPC Mixtures.** Results for the SAXS of DOPC:DOPE and DOPC:LysoPC mixtures are presented in Figure 3 and Figure 4. Samples were all hydrated at 70% (w/w) in water and buffer, which is above the excess hydration point for both systems. All samples were measured at 5, 14, 24, and 34 °C, a relevant temperature range for protein reconstitution assays. Both sets of results are the mean of two independent measurements. In summary, all of the samples measured during these SAXS studies showed that the phase behavior of the phospholipids was lamellar. Micellar phases can also be detected with SAXS;

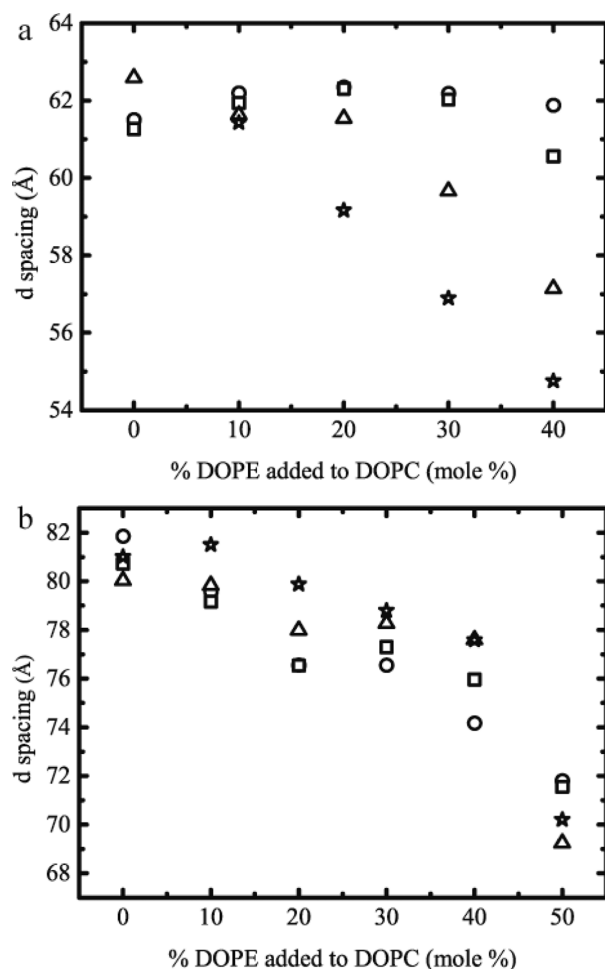


**Figure 3.** SAXS data showing the effect on layer spacing of increasing mol % of DOPE when added to a DOPC system in (a) MQ water and (b) buffer (20 mM HEPES, 100 mM KCl, 0.5 M sucrose) for (○) 5 °C, (□) 14 °C, (△) 24 °C, and (☆) 34 °C. Both data sets were hydrated above 70% (w/w). The temperature range reflects a normal range used for protein reconstitution and activity measurements. Error bars are of the order of the data points.

however, the signal is generally swamped by the lamellar signals, hence the use of  $^{31}\text{P}$  NMR discussed later.

**1. DOPC:DOPE Mixtures.** As shown in Figure 3, DOPC:DOPE systems in both water and buffer generally show a decrease in layer spacing with increasing amounts of DOPE. For samples hydrated in water (Figure 3a), the change in layer spacing is temperature dependent, showing a greater decrease in lattice parameter at higher temperatures. At 5 and 14 °C, very little change is seen in the water samples, with changes of only a few angstroms noted above a DOPE concentration of 30 mol %. In this study, DOPC and DOPE molecules were chosen with identical chain lengths so that the molecules only differed in the headgroup region, and hence, chain length considerations and their effects on layer spacing are not discussed. One specific property of a PE headgroup is its ability to form direct phosphate-ammonium intermolecular dipolar interactions with other PE headgroups.<sup>27</sup> In comparison, PC is unable to form these because of the lack of an amine donor moiety.<sup>28</sup> When increasing amounts of DOPE are added to a DOPC bilayer, the level of intramolecular hydrogen bonding within the bilayer increases,<sup>27</sup> resulting in a decrease in layer spacing as observed.

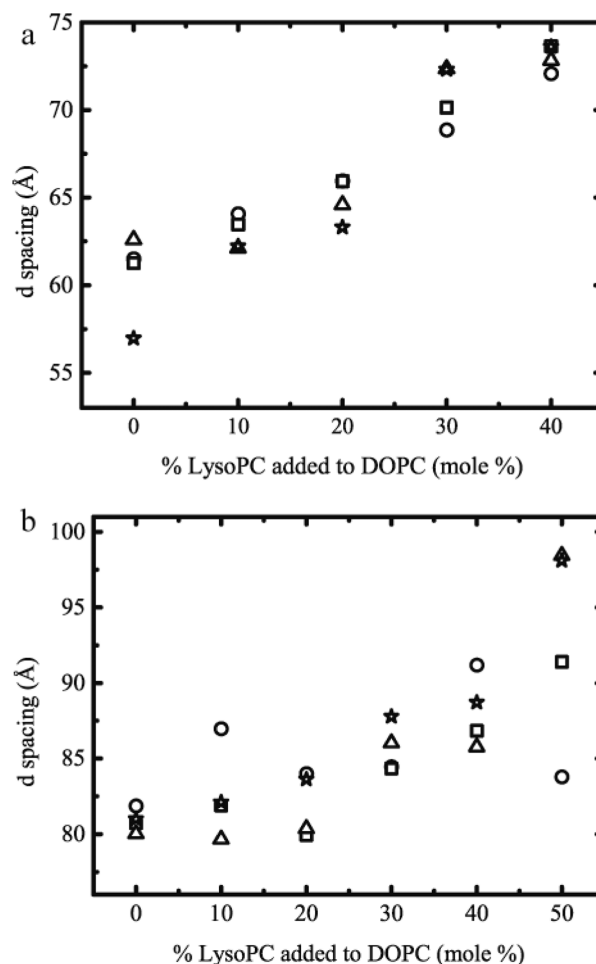


**Figure 4.** SAXS data showing the effect on layer spacing of increasing mol % of LysoPC when added to a DOPC system in (a) MQ water and (b) buffer (20 mM HEPES, 100 mM KCl, 0.5 M sucrose) for (○) 5 °C, (□) 14 °C, (△) 24 °C, and (☆) 34 °C. Both data sets were hydrated above 70% (w/w). The temperature range reflects a normal range used for protein reconstitution and activity measurements. Error bars are of the order of the data points.

As temperature increased, layer spacing decreased for all the DOPC:DOPE mixtures. This effect was particularly prominent in the samples hydrated in water shown in Figure 3a, in comparison to those hydrated in buffer shown in Figure 3b. At higher temperatures, DOPE is known to adopt a hexagonal phase over a wide range of hydrations.<sup>29</sup> Previous studies have shown that the volume of the headgroup is independent of hydrocarbon chain length and temperature<sup>30</sup> and that the volume occupied by the hydrocarbon chains increases with increasing temperature. Increased volume leads to greater conformational disorder in the hydrocarbon chains and a lateral expansion of the acyl chain region in comparison to the headgroup region. As the phase-transition temperature is approached, the increased lateral expansion will reduce the layer spacing as observed because of the hydrogen bonding and van der Waals forces dominating. Eventually, the increased curvature frustration in the chain region will lead to a phase change, but this was not observed in these compositions.

The effect of temperature is altered by the presence of buffer as seen in Figure 3b, as is the overall layer spacing which is at least 15 Å higher in the buffered system. Previous studies have shown that the presence of salts can disrupt the hydrogen bond



network in solvating water,<sup>31</sup> either promoting or reducing hydrogen bonding, depending on the anion, cation, and charge density. The buffer used in these studies contained both KCl and HEPES, and so while the system is not directly comparable to these studies, it is of note that the hydrogen bonding within the solvating medium may have been altered. In this case, this observed increase in layer spacing suggests that the presence of the buffer may be promoting hydrogen bonding and partially contributing to the increase in layer spacing.

It is already known that there is no significant binding of monovalent ions to PC and PE bilayers, and therefore, no effects can be attributed to long-range repulsions between bilayers.<sup>32</sup> Attractive van der Waals forces have been shown to be reduced by the addition of salt solutions, as the electrostatic contribution to them is screened out when the interbilayer separation is much greater than the Debye screening length.<sup>33</sup> This could be another explanation for the increased layer spacing seen in the buffered system.

The addition of small monosaccharide sugars such as glucose and fructose has also been shown to swell bilayers which are in excess hydration.<sup>34</sup> The mechanism for this has been subject to some discussion; however, we propose that the combination of this and the reduction in attractive van der Waals forces, as well as a possible influence on hydrogen bonding, causes the significant swelling seen in buffer in comparison to water. We would expect the swelling due to the addition of sugar and the change in van der Waals forces to be temperature independent and to dominate the system, mitigating effects such as changes in hydrogen bonding, seen in the reduced sensitivity to temperature in the buffered system in comparison to the water system.

**2. DOPC:LysoPC Mixtures.** Both the water and buffer systems shown in Figure 4a and b show an increase in layer spacing for increasing concentrations of LysoPC added to a DOPC bilayer. The presence of lysophospholipids in a DOPC bilayer leads to reduced hydrophobicity in the hydrocarbon tail region<sup>10</sup> because of the smaller number of hydrocarbon chains (one vs two) present per headgroup upon the addition of LysoPC. Reducing the hydrophobic effect enables the bilayers to swell to greater layer spacings as the repulsive forces between bilayers will dominate over the hydrophobicity. This provides a mechanism to explain the increase in layer spacing observed for increasing LysoPC concentrations.

There is little effect over the temperature range studied in both the water and buffer cases, again suggesting that hydrophobic interactions dominate rather than more temperature-dependent effects such as hydrocarbon chain volume as observed in the DOPC:DOPE sample.

Of note is that the buffer system shown in Figure 4b undergoes a similar change in swelling (approximately 15 Å) over the same compositional changes as the water system in Figure 4a. The explanation of reduced hydrophobicity is therefore strengthened as this would not be affected by the hydrating medium as observed. However, as observed in Figure 3 with DOPC:DOPE mixtures, the buffered system exhibits a greater layer spacing than the water system, with the increase in both cases between the water and buffer systems of a similar magnitude. This implies the same mechanism in both systems which we attribute to the reduction of the attractive van der Waals by electrostatic screening and the presence of sucrose as discussed previously. This result agrees well with previous studies which also reported an increase in lattice parameter with

increasing buffer, attributed to membrane–buffer interactions leading to a downstream bilayer softening.<sup>13</sup>

### **<sup>31</sup>P Static NMR Studies of DOPC:LysoPC Mixtures.**

Solid state <sup>31</sup>P static NMR experiments were undertaken for DOPC:LysoPC multilamellar vesicle (MLV) combinations in both water and buffer systems at 4 °C. The results show a characteristic <sup>31</sup>P NMR pattern which is dominated by chemical shift anisotropy (CSA).<sup>35</sup> Results confirmed that all of the samples were predominantly lamellar which agrees with the SAXS data; however, some samples also exhibited an isotropic peak. Therefore, line shapes were subsequently fitted to extract the different powder patterns, chemical shift, and distortion of the lipid samples in the magnetic field, the results for which are presented and discussed in the subsequent section.

**1. Analysis of Isotropic Content of Samples.** Results for the <sup>31</sup>P static solid state NMR experiments performed on the DOPC:LysoPC compositions in water and buffer at 4 °C are displayed in Figure 5. All the spectra have been normalized so that their integral is equal to one in order to allow proper comparison.

As a general trend, in buffer, line widths shown in Figure 5b are slightly broader than the water ones. All these measurements have been repeated and are in good agreement with each other. For samples containing 30 mol % of LysoPC and above, a small isotropic peak centered at 0 ppm can be seen in both the water and buffer samples. Micelles exhibit rapid tumbling in a sample, resulting in motional averaging and a sharp isotropic peak centered at 0 ppm. This averaging also occurs to some extent for small vesicles, with the line width of the isotropic peak increasing with increasing vesicle size up to a vesicle radius of 1500 Å, after which the spectrum becomes asymmetrical.<sup>36</sup> Previous studies have demonstrated micellar line widths of 1–2 ppm;<sup>37</sup> however, the line width of the isotropic peak observed in the DOPC:LysoPC mixtures is approximately 8–9 ppm, indicating a vesicle size of ca. 1000–1500 Å. Pure LysoPC has a low critical micelle concentration (CMC) and a propensity for micelle formation.<sup>38</sup> This isotropic peak suggests that small unilamellar vesicles (SUVs) are effectively budding off from the main bulk sample creating two populations of lipid vesicles, a small one and a large one. Similar budding behavior has been reported in giant unilamellar vesicles composed of dipalmitoylphosphatidylcholine and cholesterol with LysoPC added to the external solution.<sup>20</sup> It is likely that these vesicles are LysoPC rich, as they are only observed above 30 mol % LysoPC, although it is not possible to unequivocally determine their composition. This population appears to be more prominent in the buffer samples and constitutes a maximum percentage of 11 mol % of the total amount of lipid. This implies that in terms of relative populations of MLVs and SUVs, a significant proportion of the sample is composed of vesicles in the lipid mixture DOPC:LysoPC 50:50. In the context of protein reconstitution studies, LysoPC has in fact been shown to stabilize small unilamellar vesicles,<sup>39</sup> and their presence implies that the evaluation of protein activity in similar lipid compositions should be treated with caution to ensure that any activity seen is due to a single population of proteins reconstituted into vesicles rather than a mixed population as observed here.

**2. Fitting of <sup>31</sup>P Static NMR Line Shapes.** The line shape of the static CSA pattern is characterized by a downfield shoulder, the  $\sigma_{\text{para}}$ , and a sharper upfield peak, the  $\sigma_{\text{perp}}$ , which results from the partial averaging of the CSA tensor because of motion within the vesicle. The  $\sigma_{\text{para}}$  and  $\sigma_{\text{perp}}$  values correspond to the

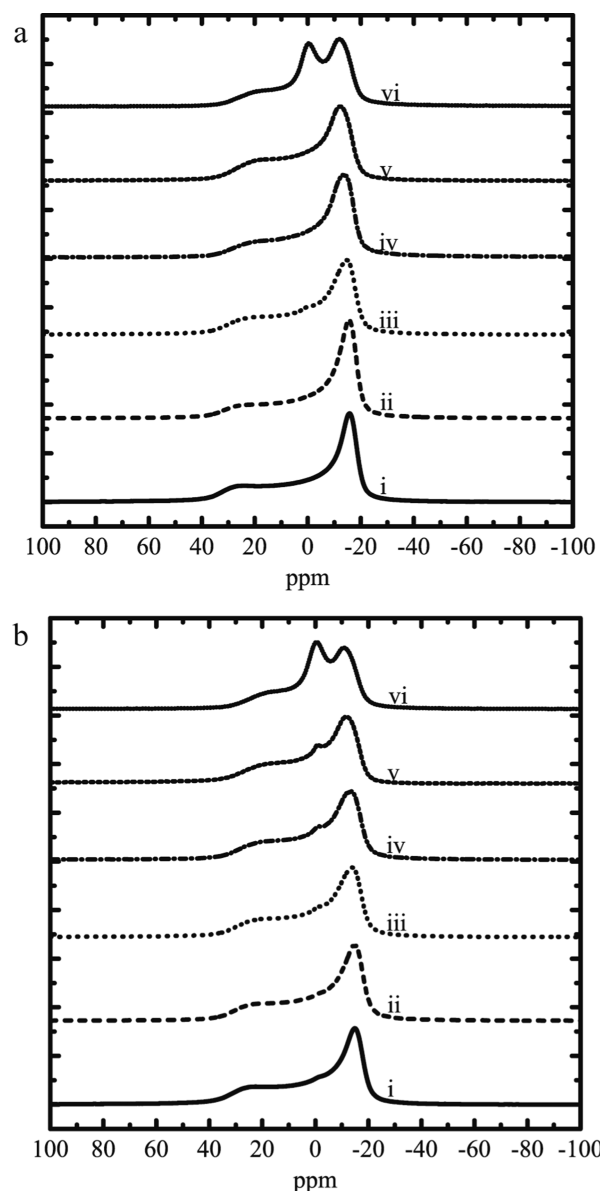


**Figure 5.**  $^{31}\text{P}$  static NMR data of DOPC:LysoPC mixtures in (a) MQ water and (b) buffer (20 mM HEPES, 10 mM KCl, 0.5 M sucrose) for DOPC:LysoPC mol % ratios of (i) 100:0, (ii) 90:10, (iii) 80:20, (iv) 70:30, (v) 60:40, and (vi) 50:50. The isotropic peak at 0 ppm constitutes <11% of the sample intensity in the 50:50 case and <1% in all other cases.

$^{31}\text{P}$  frequencies of the bilayers with their normals either parallel or perpendicular, respectively, relative to the direction of the applied magnetic field.<sup>24</sup>

After fitting the raw data, plots were made of the parameters extracted from the fits  $\sigma_{\text{para}}$ ,  $\sigma_{\text{perp}}$ , and  $c/a$  which are shown in Figure 6 and Figure 7. In these plots, each point represents the mean of two independent samples and fits. Figure 6 shows a clear decrease in both  $\sigma_{\text{para}}$  and  $\sigma_{\text{perp}}$  for increasing amounts of LysoPC. For  $\sigma_{\text{para}}$ , the values for the buffer samples are generally larger than for the water samples, while for  $\sigma_{\text{perp}}$ , the values for the buffer samples are consistently smaller than those of the water ones, although both still follow the same downward trend. One potential reason for this is that the salts within the buffer are affecting the local electronic environment of the phosphorus headgroups and altering the

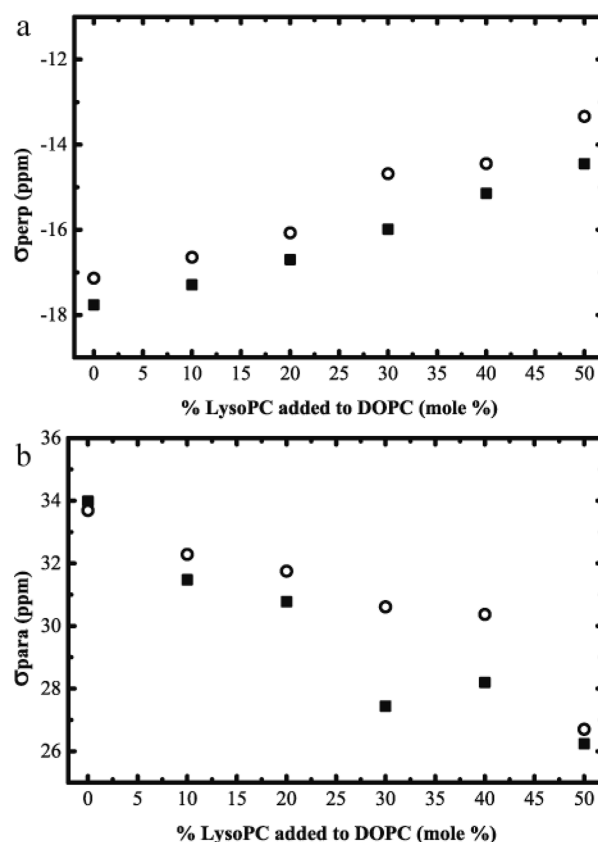


**Figure 6.** Data extracted from fitting  $^{31}\text{P}$  static NMR data showing the change in chemical shift of the samples of DOPC:LysoPC mixtures in (■) water and (○) buffer (20 mM HEPES, 100 mM KCl, 0.5 M sucrose) broken down into (a) perpendicular component and (b) parallel component.

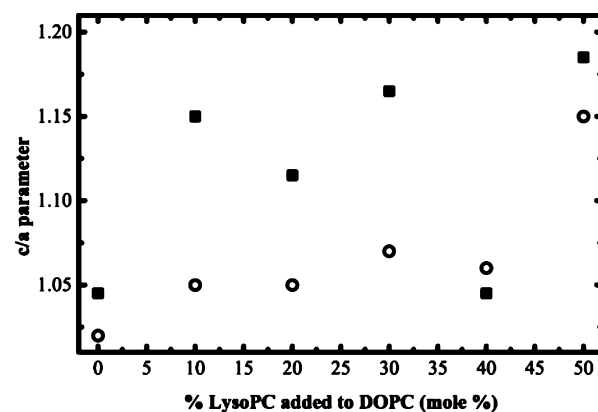


**Figure 7.** Data showing the distortion of the DOPC:LysoPC mixtures in the magnetic field, extracted from the fits and shown in terms of the  $c/a$  parameter (Figure 2) for both (■) water and (○) buffer (20 mM HEPES, 100 mM KCl, 0.5 M sucrose). The results for water and buffer are the mean of two independent sets of measurements. A global average for water and buffer with error bars can be seen in Figure S3 of the Supporting Information.

CSA; however, the effects of this are small. The decrease in the CSA for increasing amounts of LysoPC added to a DOPC membrane is as expected. LysoPC molecules are able to undergo faster rapid motion about the lipid headgroup because of increased motional freedom of the headgroup about the glycerol C2–C3 bond in comparison to DOPC molecules. This

leads to an averaging and a subsequent reduction in the observed CSA.<sup>40,41</sup> This information helps to confirm the accuracy and reliability of the experiments and gives further weight to the data presented in the next section.

**3. Analysis of Distortion in the Magnetic Field of Lipids.** Figure 7 shows the  $c/a$  data extracted from the fits to the solid-state NMR data. This parameter reflects the distortion of the lipid vesicles in the magnetic field as it is the average ratio between the two perpendicular axes of the vesicle. Both the water and buffer samples show a general upward trend in the  $c/a$  parameter for increasing amounts of LysoPC added to a DOPC bilayer.

It has already been well documented that adding LysoPC to a DOPC bilayer has implications for membrane stability, and sufficiently high concentrations of LysoPC can lead to a breakdown of the bilayer to form mixed micelles.<sup>42</sup> Hence, it would be expected that vesicles containing a higher content of LysoPC would be more susceptible to deformation as a result of an applied magnetic field. The slight reduction in buffer as opposed to water could also be explained if the buffer were causing an additional electronic shielding effect, hence reducing the CSA and subsequently the deformation. An unexpected result was seen for the lipid combination DOPC:LysoPC 60:40 mol % where the  $c/a$  parameter does not follow the upward trend, most notably in the samples hydrated in water. There is no abnormality in the chemical shift at this composition. A reduction in the  $c/a$  parameter implies that, at this composition, the lipids are less susceptible to deformation. This drop in the  $c/a$  parameter cannot be explained in terms of spontaneous curvature as then it would be expected for the DOPC:LysoPC 50:50 sample as well. At a composition of DOPC:LysoPC 50:50, the NMR data shows a mixed population of lipids with up to 11 mol % of the sample comprising SUVs in addition to the MLVs. Prior to this, the proportion of SUVs is <1 mol %. This implies that the DOPC:LysoPC 60:40 composition may be close to a saturation point for the amount of LysoPC that can be incorporated in a stable DOPC membrane and that around this point there is a change in the flexibility of the membrane. After the saturation point, the membrane would be less stable, significant vesicle budding occurs, and the relative compositions of the MLVs and SUVs cannot be determined, and hence, the  $c/a$  parameter reflects a mixture of populations. It is also possible that this saturation point will vary slightly in water and buffer, hence the differences in the magnitude of the change in the  $c/a$  parameter. This is justified by the increased proportion of SUVs in the DOPC:LysoPC 60:40 mol % buffer sample in comparison to the water sample.

The results in Figure 7 for concentrations of LysoPC around 40 mol % are particularly exciting when compared to a preliminary data set obtained for a mechanosensitive channel activity in extruded vesicles of the same compositions presented in this paper. In those activity results, an increase in mechanosensitive channel activity was seen for the lipid combination DOPC:LysoPC 60:40, which was very close to the activity recorded for the DOPC sample. This appears to correlate with the results obtained from the solid-state NMR fitting which showed a change in the  $c/a$  parameter for the same lipid composition. As this was seen for both the water and buffer systems, we propose that the effect seen is due to a distinct membrane property rather than to just a buffer effect. These results document a change in protein activity which can preliminarily be correlated back to distinct membrane biophysical measurements. While it is not possible to speculate

exactly which membrane parameter might be causing these changes from the solid-state NMR results, it opens the door for further investigations and insight into how fundamental membrane properties can affect membrane proteins like mechanosensitive channels. At higher compositions of LysoPC, the activity due to the mixed populations of lipids cannot be uniquely determined from the change in composition. This correlation is currently the subject of further investigations.

## CONCLUSIONS

We investigated lipid mixtures of dioleoylphosphatidylcholine (DOPC), dioleoylphosphatidylethanolamine (DOPE), and lysophosphatidylcholine (LysoPC) examining their behaviors in excess water and buffer systems over the temperature range 4–34 °C. These combinations are commonly used to investigate the effects of spontaneous curvature on integral membrane proteins reconstituted into vesicles of these compositions. The temperature range is also reflective of common protein reconstitution methods.<sup>14–17</sup> We showed that all of the lipid compositions studied were lamellar with some samples showing an additional vesicle content, in both water and buffer, making them suitable candidates for protein reconstitution studies.

Changes in layer spacing were measured for all the lipid mixtures, showing that the swelling of the bilayers varies significantly dependent on the buffer and the lipid composition. The buffer caused additional swelling in both lipid mixtures, thought to be due to the screening of attractive van der Waals forces and the addition of sucrose. While layer spacing obtained from SAXS incorporates the interbilayer water as well as the bilayer width and is therefore not a specific determination of variations in bilayer width, hydrophobic mismatch is one of the causes known to decrease protein activity.<sup>2,43</sup> Therefore, variations caused by compositional and hydration media must be considered rather than solely chain length for optimization of protein activity experiments reconstituted into lipid bilayers. This highlights the need for careful consideration of buffers and sugars when working with lipid mixtures for protein assays, even for uncharged lipid systems.

<sup>31</sup>P static NMR performed on the DOPC:LysoPC mixtures showed the presence of SUV populations for 60:40 and 50:50 (mol %) mixtures. The presence of SUVs could affect the solvation of any proteins studied in these mixtures as well as further activity measurements.

During the fitting of the <sup>31</sup>P static NMR line shapes, it was discovered that DOPC:LysoPC mixtures show a nonlinear distortion in the magnetic field with a discontinuity at a ratio of 60:40 (mol %). This implies an underlying flexibility in the membrane at this composition and that consideration of spontaneous curvature alone when investigating the effects of membrane tension may not be sufficient.

This research highlights how seemingly small variations in lipid systems can affect biophysical membrane properties and shows how fundamental membrane measurements are crucial to the interpretation of lipid–protein activity assays.

## ASSOCIATED CONTENT

### Supporting Information

Example X-ray images showing DOPC:DOPE and DOPC:LysoPC at differing temperatures, example fits showing the <sup>31</sup>P NMR data and the simulated fits for water samples of DOPC:LysoPC mixtures, data showing the mean distortion of the DOPC:LysoPC mixtures in the magnetic field, extracted



from the water and buffer fits and shown in terms of the  $c/a$  parameter. This material is available free of charge via the Internet at <http://pubs.acs.org>.

## AUTHOR INFORMATION

### Corresponding Authors

\*E-mail: [r.law@imperial.ac.uk](mailto:r.law@imperial.ac.uk).

\*E-mail: [o.ces@imperial.ac.uk](mailto:o.ces@imperial.ac.uk).

### Author Contributions

The manuscript was written through contributions of all authors. All authors have given approval to the final version of the manuscript.

### Notes

The authors declare no competing financial interest.

## ACKNOWLEDGMENTS

This work was supported by the EPSRC via grant EP/G00465X/1 and by an EPSRC Centre for Doctoral Training Studentship from the Institute of Chemical Biology (Imperial College London) part funded by Pfizer Global Research and Development via grant EP/F500076/1 awarded to Hanna Barriga. We acknowledge the European Synchrotron Radiation Facility for provision of synchrotron beamtime and we would like to thank Dr Michael Sztucki for assistance using beamline ID02.

## ABBREVIATIONS

NMR, nuclear magnetic resonance; DOPC, dioleoylphosphatidylcholine; DOPE, dioleoylphosphatidylethanolamine; LysoPC, lysophosphatidylcholine

## REFERENCES

- (1) Spector, A. A.; Yorek, M. A. Membrane lipid composition and cellular function. *J. Lipid Res.* **1985**, *26*, 1015–1035.
- (2) Pilot, J. D.; East, J. M.; Lee, A. G. Effects of Bilayer Thickness on the Activity of Diacylglycerol Kinase of *Escherichia coli*. *Biochemistry* **2001**, *40* (28), 8188–8195.
- (3) Pilot, J. D.; East, J. M.; Lee, A. G. Effects of Phospholipid Headgroup and Phase on the Activity of Diacylglycerol Kinase of *Escherichia coli*. *Biochemistry* **2001**, *40* (49), 14891–14897.
- (4) Curran, A. R.; Templer, R. H.; Booth, P. J. Modulation of Folding and Assembly of the Membrane Protein Bacteriorhodopsin by Intermolecular Forces within the Lipid Bilayer. *Biochemistry* **1999**, *38*, 9328–9336.
- (5) Ces, O.; Mulet, X. Physical coupling between lipids and proteins: a paradigm for cellular control. *Signal Transduction* **2006**, *6* (2), 112–132.
- (6) Attard, G. S.; Templer, R. H.; Smith, W. S.; Hunt, A. N.; Jackowski, S. Modulation of CTP:phosphocholine cytidyltransferase by membrane curvature elastic stress. *Proc. Natl. Acad. Sci. U.S.A.* **2000**, *97* (16), 9032–9036.
- (7) Gawrisch, K.; Parsegian, V. A.; Hajduk, D. A.; Tate, M. W.; Gruner, S. M.; Fuller, N. L.; Rand, R. P. Energetics of a Hexagonal-Lamellar-Hexagonal Phase Transition Sequence in Dioleoylphosphatidylethanolamine Membranes. *Biochemistry* **1992**, *31*, 2856–2864.
- (8) Fuller, N. L.; Rand, R. P. The Influence of Lysolipids on the Spontaneous Curvature and Bending Elasticity of Phospholipid Membranes. *Biophys. J.* **2001**, *81*, 243–254.
- (9) Zimmerberg, J.; Gawrisch, K. The Physical Chemistry of Biological Membranes. *Nat. Chem. Biol.* **2006**, *2* (11), 564–567.
- (10) Costigan, S. C.; Booth, P. J.; Templer, R. H. Estimations of Lipid Bilayer Geometry in Fluid Lamellar Phases. *Biochim. Biophys. Acta* **2000**, *1468* (1–2), 41–54.
- (11) Claessens, M. M.; van Oort, B. F.; Leermakers, F. A.; Hoekstra, F. A.; Cohen Stuart, M. A. Charged lipid vesicles: effects of salts on bending rigidity, stability, and size. *Biophys. J.* **2004**, *87* (6), 3882–3893.
- (12) Bouvrais, H.; Duelund, L.; Ipsen, J. H. Buffers affect the bending rigidity of model lipid membranes. *Langmuir* **2014**, *30* (1), 13–16.
- (13) Peiro-Salvador, T.; Ces, O.; Templer, R. H.; Seddon, A. M. Buffers may adversely affect model lipid membranes: a cautionary tale. *Biochemistry* **2009**, *48* (47), 11149–11151.
- (14) Rigaud, J. L. Membrane proteins: functional and structural studies using reconstituted proteoliposomes and 2-D crystals. *Braz. J. Med. Biol. Res.* **2002**, *35*, 753–766.
- (15) Battle, A. R.; Petrov, E.; Pal, P.; Martinac, B. Rapid and improved reconstitution of bacterial mechanosensitive ion channel proteins MscS and MscL into liposomes using a modified sucrose method. *FEBS Lett.* **2009**, *583* (2), 407–412.
- (16) Knol, J.; Sjollem, K.; Poolman, B. Detergent-Mediated Reconstitution of Membrane Proteins. *Biochemistry* **1998**, *37*, 16410–16415.
- (17) Gorzelle, B. M.; Nagy, J. K.; Oxenoid, K.; Lonzer, W. L.; Cafiso, D. S.; Sanders, C. R. Reconstitutive Refolding of Diacylglycerol Kinase, an Integral Membrane Protein. *Biochemistry* **1999**, *38* (49), 16373–16382.
- (18) Marsh, D. Lateral pressure profile, spontaneous curvature frustration, and the incorporation and conformation of proteins in membranes. *Biophys. J.* **2007**, *93* (11), 3884–3899.
- (19) Powl, A. M.; East, J. M.; Lee, A. G. Anionic Phospholipids Affect the Rate and Extent of Flux through the Mechanosensitive Channel of Large Conductance MscL. *Biochemistry* **2008**, *47*, 4317–4328.
- (20) Tanaka, T.; Ryoko, S.; Yamashita, Y.; Yamazaki, M. Shape changes and vesicle fission of giant unilamellar vesicles of liquid-ordered phase membrane induced by lysophosphatidylcholine. *Langmuir* **2004**, *20*, 9526–9534.
- (21) Coey, A. T.; Sahu, I. D.; Gunasekera, T. S.; Troxel, K. R.; Hawn, J. M.; Swartz, M. S.; Wickenheiser, M. R.; Reid, R. J.; Welch, R. C.; Vanoye, C. G.; Kang, C.; Sanders, C. R.; Lorigan, G. A. Reconstitution of KCNE1 into lipid bilayers: comparing the structural, dynamic, and activity differences in micelle and vesicle environments. *Biochemistry* **2011**, *50* (50), 10851–10859.
- (22) Warschawski, D. E.; Arnold, A. A.; Beaugrand, M.; Gravel, A.; Chartrand, E.; Marcotte, I. Choosing membrane mimetics for NMR structural studies of transmembrane proteins. *Biochim. Biophys. Acta* **2011**, *1808* (8), 1957–1974.
- (23) Perozo, E.; Kloda, A.; Cortes, D. M.; Martinac, B. Physical principles underlying the transduction of bilayer deformation forces during mechanosensitive channel gating. *Nat. Struct. Biol.* **2002**, *9* (9), 696–703.
- (24) Dubinnyi, M. A.; Lesovoy, D. M.; Dubovskii, P. V.; Chupin, V. V.; Arseniev, A. S. Modeling of <sup>31</sup>P-NMR spectra of magnetically oriented phospholipid liposomes: A new analytical solution. *Solid State Nucl. Magn. Reson.* **2006**, *29* (4), 305–311.
- (25) Picard, F.; Paquet, M. J.; Levesque, J.; Belanger, A.; Auger, M. <sup>31</sup>P NMR First Spectral Moment Study of the Partial Magnetic Orientation of Phospholipid Membranes. *Biophys. J.* **1999**, *77*, 888–902.
- (26) Marquardt, D. W. An algorithm for least squares estimation of nonlinear parameters. *J. Soc. Ind. Appl. Math.* **1963**, *11* (2), 431–441.
- (27) Hubner, W.; Blume, A. Interactions at the lipid-water interface. *Chem. Phys. Lipids* **1998**, *96*, 99–123.
- (28) Orsi, M.; Essex, J. W. Physical properties of mixed bilayers containing lamellar and non lamellar lipids: insights from coarse-grain molecular dynamics simulations. *Faraday Discuss.* **2013**, *161*, 249–272.
- (29) Seddon, J. M.; Templer, R. H. Polymorphism of lipid water systems. In *Handbook of Biological Physics*; Hoff, Lipowsky, Sackmann, Eds.; Elsevier: Amsterdam, 1995; Chapter 3, Vol. 1, pp 97–160.
- (30) Wilkinson, D. A.; Nagle, J. F. Dilatometry and Calorimetry of Saturated Phosphatidylethanolamine Dispersions. *Biochemistry* **1981**, *20* (1), 187–192.
- (31) Nucci, N. V.; Vanderkooi, J. M. Effects of Salts of the Hofmeister Series on the Hydrogen Bond Network of Water. *J. Mol. Liq.* **2008**, *143* (2–3), 160–170.



- (32) Marra, J.; Israelachvili, J. Direct Measurement of Forces between Phosphatidylcholine and Phosphatidylethanolamine Bilayers in Aqueous Electrolyte Solutions. *Biochemistry* **1985**, *24*, 4608–4618.
- (33) Israelachvili, J. *Intermolecular and Surface Forces*; Elsevier: Amsterdam, 2011.
- (34) Demé, B.; Zemb, T. Hydration forces between bilayers in the presence of dissolved or surface-linked sugars. *Curr. Opin. Colloid Interface Sci.* **2011**, *16* (6), 584–591.
- (35) Seelig, J. 31P Nuclear Magnetic Resonance and the Headgroup Structure of Phospholipids in Membranes. *Biochim. Biophys. Acta* **1978**, *515* (2), 105–140.
- (36) Burnell, E. E.; Cullis, P. R.; De Kruijff, B. Effects of tumbling and lateral diffusion on phosphatidylcholine model membrane 31P NMR lineshapes. *Biochim. Biophys. Acta* **1980**, *603*, 63–69.
- (37) Baciú, M.; Sebai, S. C.; Ces, O.; Mulet, X.; Clarke, J. A.; Shearman, G. C.; Law, R. V.; Templer, R. H.; Plisson, C.; Parker, C. A.; Gee, A. Degradative transport of cationic amphiphilic drugs across phospholipid bilayers. *Philos. Trans. R. Soc., A* **2006**, *364*, 2597–2614.
- (38) Kumar, V. V. Complementary Molecular Shapes and Additivity of the Packing Parameter of Lipids. *Proc. Natl. Acad. Sci. U.S.A.* **1991**, *88*, 444–448.
- (39) Kumar, V. V.; Malewicz, B.; Baumann, W. J. Lysophosphatidylcholine Stabilizes Small Unilamellar Phosphatidylcholine Vesicles. *Biophys. J.* **1989**, *55*, 789–792.
- (40) Aranda, F. J.; Killian, J. A.; de Kruijff, B. Importance of the Tryptophans of Gramicidin for its Lipid Structure Modulating Activity in Lysophosphatidylcholine and Phosphatidylethanolamine Model Membranes. *Biochim. Biophys. Acta* **1987**, *901*, 217–228.
- (41) Wu, W.; Stephenson, F. A.; Mason, J. T.; Huang, C. A Nuclear Magnetic Resonance Spectroscopic Investigation of the Headgroup Motions of Lysophospholipids in Bilayers. *Lipids* **1984**, *19* (1), 68–71.
- (42) Morris, D. A.; McNeil, R.; Castellino, F. J.; Thomas, J. K. Interaction of Lysophosphatidylcholine with Phosphatidylcholine Bilayers: A Photophysical and NMR Study. *Biochim. Biophys. Acta* **1980**, *599*, 380–390.
- (43) Powl, A. M.; East, J. M.; Lee, A. G. Different effects of lipid chain length on the two sides of a membrane and the lipid annulus of MscL. *Biophys. J.* **2007**, *93* (1), 113–122.